

12-1-2006

# AC Conductivity Relaxation Processes in $\text{CaCu}_3\text{Ti}_4\text{O}_{12}$ Ceramics: Grain Boundary and Domain Boundary Effects

Wei Li

Robert W. Schwartz

Missouri University of Science and Technology, [rschwartz@mst.edu](mailto:rschwartz@mst.edu)

Follow this and additional works at: [http://scholarsmine.mst.edu/matsci\\_eng\\_facwork](http://scholarsmine.mst.edu/matsci_eng_facwork)



Part of the [Materials Science and Engineering Commons](#)

---

## Recommended Citation

W. Li and R. W. Schwartz, "AC Conductivity Relaxation Processes in  $\text{CaCu}_3\text{Ti}_4\text{O}_{12}$  Ceramics: Grain Boundary and Domain Boundary Effects," *Applied Physics Letters*, American Institute of Physics (AIP), Dec 2006.

The definitive version is available at <http://dx.doi.org/10.1063/1.2405382>

This Article - Journal is brought to you for free and open access by Scholars' Mine. It has been accepted for inclusion in Materials Science and Engineering Faculty Research & Creative Works by an authorized administrator of Scholars' Mine. This work is protected by U. S. Copyright Law. Unauthorized use including reproduction for redistribution requires the permission of the copyright holder. For more information, please contact [scholarsmine@mst.edu](mailto:scholarsmine@mst.edu).

# ac conductivity relaxation processes in $\text{CaCu}_3\text{Ti}_4\text{O}_{12}$ ceramics: Grain boundary and domain boundary effects

Wei Li and Robert W. Schwartz<sup>a)</sup>*Department of Material Science and Engineering, University of Missouri-Rolla, Rolla, Missouri 65409*

(Received 15 August 2006; accepted 8 November 2006; published online 12 December 2006)

The ac conductivity of  $\text{CaCu}_3\text{Ti}_4\text{O}_{12}$  ceramics associated with electrical charge carrier motion (ions or vacancies) was investigated as a function of frequency at different temperatures. The long range migration of charge carriers within the ceramic is restricted by two kinds of insulating barriers, namely, grain boundaries and domain boundaries. The potential barriers associated with these boundaries lead to two anomalies in conductivity response and three frequency-dependent contributions to conductivity: long range diffusion of carriers, carrier migration localized within grains, and carrier migration localized within domains. © 2006 American Institute of Physics.

[DOI: 10.1063/1.2405382]

Over the past few years, the perovskite-related material  $\text{CaCu}_3\text{Ti}_4\text{O}_{12}$  (CCTO) has gained considerable interest due to its high ( $>10\,000$ ) and almost temperature-independent dielectric constant at elevated temperatures, as well as the steplike decrease by almost three orders of magnitude at  $\sim 100$  K. In order to understand this unique response, investigators have studied a variety of characteristics of these materials. High-resolution x-ray and neutron powder diffractions have revealed that neither a phase transition nor a detectable change of crystal structure contributes to the observed behavior.<sup>1,2</sup> Researchers gradually revealed that the high permittivity of CCTO was related to the presence of grain boundaries in ceramics<sup>3</sup> or twin boundaries in single crystals<sup>4</sup> rather than being due to an intrinsic contribution. Therefore, the characterization of grain boundaries, as well as relaxation processes associated with grain and grain boundaries, becomes extremely important.

ac conductivity measurements lend insight into different relaxation mechanisms and provide a straightforward method to separate contributing factors (grain, grain boundary, electrode, etc.) through their frequency and/or temperature-dependent response characteristics. An understanding of ac conduction mechanisms can delineate the contributions of grain and grain boundaries to the overall electrical conductivity. Unfortunately, only a few studies have focused on the ac conductivity response of these materials to characterize relaxation processes, which are closely related to the formation of high permittivity in CCTO ceramics.

In this letter, the measurement of ac conductivity for CCTO ceramics is reported. The relaxation behavior of electrical charge carrier migration from long range diffusion to localized motion is illustrated based on the characterization of two relaxation processes associated with grain boundaries and domain boundaries.

A standard mixed oxide process was used to prepare CCTO pellets that were densified by cold isostatic pressing at pressures up to 300 MPa. These pellets were then sintered at temperatures between 1040 and 1120 °C. Crystal structure and phase purity were characterized by x-ray diffraction. Impedance data were collected by a Solartron 1255B imped-

ance analyzer. The frequency and temperature ranges investigated were 1 Hz–1 MHz and 25–300 °C, respectively. The values of ac conductivity were derived from the complex impedance data using

$$\sigma' = \left[ \frac{Z'}{Z'^2 + Z''^2} \right] \times \left( \frac{t}{A} \right) = \omega \epsilon_0 \epsilon'' \quad (1)$$

where  $\sigma'$  is the ac conductivity,  $Z'$  and  $Z''$  are the real and imaginary parts of the impedance, respectively,  $t$  is the thickness, and  $A$  is the area of the CCTO capacitor.

As illustrated in the inset of Fig. 1 a typical conductivity-frequency spectrum is divided into three parts. In region 1, according to the jump relaxation model,<sup>5</sup> since the frequency is low and the electric field cannot perturb the hopping conduction mechanism of charged particles, the conductance is approximately equal to the dc value and the conduction mechanism is the same as that for dc conduction, i.e., hopping of charged particles from one localized site to another. The conductivity begins to increase nonlinearly after the frequency exceeds the critical frequency  $f_c$  in region 2

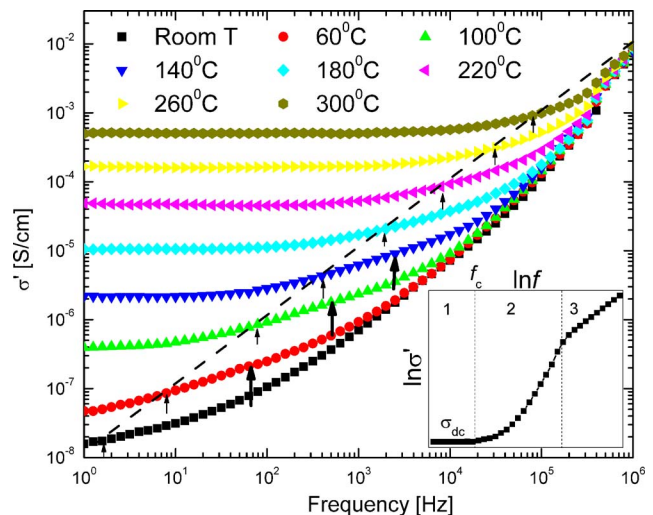


FIG. 1. (Color online) ac conductivity as a function of frequency at various temperatures for CCTO ceramics with smaller grain size. The inset shows a typical conductivity spectrum of oxide materials. The large arrows indicate anomaly frequency identified by visual inspection; small arrows indicate anomaly frequency identified by  $Z'$  and  $M''$  peaks.

<sup>a)</sup> Author to whom correspondence should be addressed; electronic mail: rwschwar@umr.edu

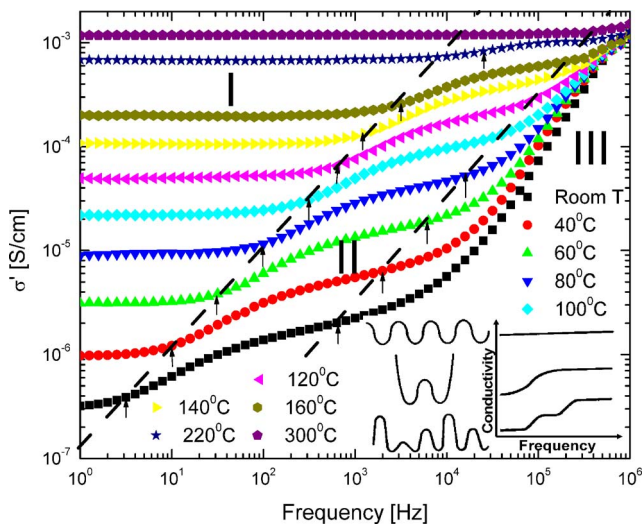


FIG. 2. (Color online) ac conductivity as a function of frequency at various temperatures for CCTO ceramics with larger grain size. The inset shows three typical potential types and their corresponding conductivity behavior. The arrows indicate anomaly frequency identified by  $Z''$  and  $M''$  peaks.

(the dispersive region) due to the fact that the capacitor admittance becomes numerically larger than the resistor admittance with increasing frequency. With further increase in frequency (region 3), conductivity becomes proportional to frequency resulting in nearly constant loss (NCL). In most materials, the NCL regime dominates the ac conductivity at high frequency or low temperature.<sup>6</sup>

Figures 1 and 2 show the variation of ac conductivity with frequency at various temperatures for CCTO ceramics with small (#1) and large (#2) grain sizes. The results that are presented in these figures and those reported in Fig. 3 below are representative of a larger number of samples prepared under sintering conditions that resulted in either small or large grain size. The log-log curves are flat in the low frequency region as the conductivity values approach those of  $\sigma_{dc}$ . As frequency increases, the curves become dispersive, as expected according to the typical spectrum shown in the inset of Fig. 1. In the high frequency regime, weak temperature dependence may be noted, and it is evident that the shapes of the curves are similar for various temperatures.

In most materials, ac conductivity due to localized states may be described by

$$\sigma' = \sigma_{dc} + Af^n, \tag{2}$$

where  $\sigma_{dc}$  is direct current conductivity and  $0 < n < 1$ . Zhang's results<sup>7</sup> indicate that the ac conductivity of CCTO cannot be described by such a formula, instead two formulas were used in different frequency regions to account for the presence of two relaxation contributions, i.e., relaxation at electrodes and grain boundaries.

Looking carefully at Fig. 1, some anomalies, indicated by the large arrows (visual inspection), can also be observed in the frequency-dependent response. These anomalies occur within the same frequency region as those reported,<sup>7</sup> suggesting the existence of multiple relaxation processes. This effect was greater for CCTO #2 (larger grain size) as shown in Fig. 2. We will demonstrate below that the low and high frequency anomalies are associated with grain boundaries and domain boundaries, respectively.

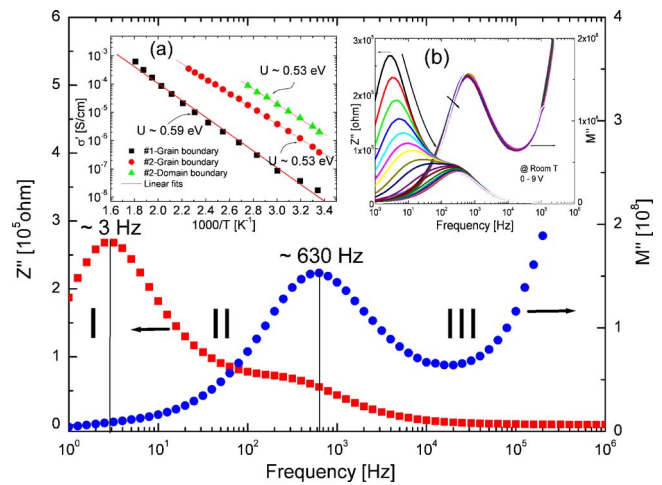


FIG. 3. (Color online) Combined  $Z''$  and  $M''$  plot of CCTO ceramics at room temperature with 0 V applied. Inset (a) shows the Arrhenius plot of the ac conductivity at the crossover frequency. Inset (b) shows the combined  $Z''$  and  $M''$  plot of CCTO at various applied voltages.

Figure 3 shows the combined  $Z''$  and  $M''$  plot of #2 at room temperature. The  $Z''$  and  $M''$  peaks should be coincident on the frequency scale and are sensitive to largest resistance and smallest capacitance, respectively.<sup>8,9</sup> Two electrical responses were observed: the first at 3 Hz (grain boundary response) and the second at 630 Hz (domain boundary response). In #1, only  $Z''$  and  $M''$  peaks corresponding to the grain boundary response (low frequency region) were found. No peaks associated with the domain boundary response were noted in impedance analysis, though very minor anomalies may be noted (large arrows) in the conductivity results of Fig. 1. Both  $Z''$  and  $M''$  peak frequencies in #1 and #2 shift to higher values with increasing temperature and have been marked by the small arrows in Figs. 1 and 2, respectively. It is interesting to note that these peak frequencies coincide with the crossover frequencies ( $f_c$ ) from dc behavior to dispersive conductivity at each temperature, and/or from one relaxation process to another (behavior more evident for #2). The value of  $f_c$  was found to be thermally activated with a similar activation energy as  $\sigma_{dc}$ . As a consequence, by connecting the crossover frequencies, we obtain straight lines with slopes close to 1, by which two (#1) and three (#2) conductivity regions are identified. The ac conductivity at the crossover frequency is plotted as a function of temperature in inset (a) of Fig. 3. The activation energy values calculated from the Arrhenius relation are close to that for the hopping of oxygen vacancies in oxide materials. Oxygen vacancies are doubly charged with respect to the neutral lattice and are considered to be the most mobile intrinsic ionic defect in these materials. A potential well picture may be employed to better understand the conductivity versus frequency behavior that is observed.

The power law dependence of conductivity on frequency [the second term in Eq. (2)] is of a universal nature and corresponds to the short range hopping of charged particles through trap sites separated by energy barriers of varied heights, as illustrated in the inset of Fig. 2. If a single charged species is presumed to move along an infinite lattice of identical potential wells (upper part inset), the conductivity is expected to be independent of frequency (in the absence of long range interactions). In the case of a single particle hopping backward and forward in a double well with AIP license or copyright; see <http://apl.aip.org/apl/copyright.jsp>

infinite barriers on either side (middle part inset), conductivity will increase and saturate at high frequency. Finally, in the case of a potential well profile with multiple barrier heights (bottom part inset), the conductivity will show multiple steplike increases as a function of frequency.<sup>10</sup>

This general picture of conduction and energy barriers is now related to the present case. There are two kinds of insulating barriers present in CCTO ceramics that can affect conductivity: domain boundaries and grain boundaries.<sup>11</sup> The presence of domain boundaries in polycrystalline CCTO materials has been confirmed.<sup>12</sup> Domains usually developed inside larger grains of CCTO (Ref. 13) and their density (number) is much larger than the density of grain boundaries. This is consistent with our observation that the domain boundary response is more prevalent in #2, which has a larger grain size compared with #1. Additionally, as shown in inset (b) of Fig. 3, both the peak heights and frequencies of the  $Z''$  and  $M''$  peaks associated with domain boundaries are independent of applied voltage, which rules out electrode effects (the capacitance of the electrode effect is a function of applied field) as the origin of the observed anomaly. Given these factors and the anticipated shorter distance between domain boundaries versus grain boundaries, it is reasonable to believe that the electric response at 630 Hz is associated with domain boundaries while the response at 3 Hz is associated with grain boundaries. Comparing the calculated activation energies for domain boundaries and grain boundaries, we may conclude that the potential barriers at grain boundaries and domain boundaries are similar. Compared to the schematic in the inset of Fig. 2, essentially a single activation energy for conduction exists in these materials, however, the differing spatial densities of domain boundaries and grain boundaries influence the mobility of the charge carriers at different frequencies. Because domain boundaries lie closer to one another than grain boundaries, the relaxation associated with these barriers occurs at a higher frequency.

Lastly, we would like to present a physical picture illustrating charge carrier relaxation behavior at various frequencies and its contributions to the overall ac conductivity. This picture may be helpful in understanding the origin of the high permittivity of CCTO and similar materials, as well as its frequency and temperature dependence. As seen in Fig. 3, the frequency response of conductivity is divided into three regimes, I, II, and III, by anomalies associated with potential barriers due to grain boundaries and domain boundaries. At the highest measurement frequencies (regime III), the highest values of conductivity are observed. At these frequencies, long range motion of carriers does not occur due to the high frequency of the bipolar applied field. The resulting short range motion of charge carriers is consequently not impacted by potential barriers associated with either domain bound-

aries or grain boundaries, and conduction is localized within individual domains. As frequency is decreased, the charge carrier moves a greater distance, until it is impeded by the potential barrier associated with a domain boundary. A corresponding decrease in conductivity occurs at this frequency, which corresponds to the onset of regime II. The conduction is then localized within individual grains instead of domains. With further decrease in frequency, grain boundaries cause an additional reduction in conductivity, at the onset of region I. Within this region, the resulting ac conductivity is close to the value of dc conductivity and the conduction is changed to a long range behavior. Therefore, the conductivity behavior is restricted by the potential barrier heights for domain boundaries and grain boundaries, the physical distance between these boundaries, and the activation energy for dc conduction. With increasing temperature, relaxation frequencies for both grain boundaries and domain boundaries shift to higher values, as influenced by the increase in carrier mobility, which results in a greater distance of motion, and increased thermal energy which is available to overcome the potential barriers. At the highest temperatures studied, conductivity becomes independent of frequency, an expected result based on the physical picture proposed. The picture presented is also consistent with the usual internal boundary layer capacitor model of CCTO materials used to explain the high permittivity of the material.

This work was supported by a MURI Program sponsored by the Office of Naval Research under Grant. No. N000-14-05-1-0541.

<sup>1</sup>A. P. Ramirez, M. A. Subramanian, M. Gardel, G. Blumberg, D. Li, T. Vogt, and S. M. Shapiro, *Solid State Commun.* **115**, 217 (2000).

<sup>2</sup>M. A. Subramanian, D. Li, N. Duan, B. A. Reisner, and A. W. Sleight, *J. Solid State Chem.* **151**, 323 (2000).

<sup>3</sup>D. C. Sinclair, T. B. Adams, F. D. Morrison, and A. R. West, *Appl. Phys. Lett.* **80**, 2153 (2002); T. B. Adams, D. C. Sinclair, and A. R. West, *Adv. Mater. (Weinheim, Ger.)* **18**, 1321 (2002).

<sup>4</sup>C. C. Homes, T. Vogt, S. M. Shapiro, S. Wakimoto, and A. P. Ramirez, *Science* **293**, 673 (2001).

<sup>5</sup>K. Funke, *Solid State Ionics* **18-19**, 183 (1986); *Prog. Solid State Chem.* **22**, 111 (1992).

<sup>6</sup>C. Leon, A. Rivera, A. Varez, J. Sanz, J. Santamaria, and K. L. Ngai, *Phys. Rev. Lett.* **86**, 1279 (2001).

<sup>7</sup>L. Zhang, *Appl. Phys. Lett.* **87**, 022907 (2005).

<sup>8</sup>D. C. Sinclair and A. R. West, *J. Appl. Phys.* **66**, 3850 (1989).

<sup>9</sup>M. A. L. Nobre and S. Lanfredi, *J. Appl. Phys.* **93**, 5576 (2003).

<sup>10</sup>E. Barsoukov and J. R. Macdonald, *Impedance Spectroscopy Theory, Experiment, and Applications* (Wiley, Hoboken, NJ, 2005), 46.

<sup>11</sup>S. F. Shao, J. L. Zhang, P. Zheng, W. L. Zhong, and C. L. Wang, *J. Appl. Phys.* **99**, 084106 (2006).

<sup>12</sup>S. Y. Chung, I. D. Kim and S. J. L. Kang, *Nat. Mater.* **3**, 774 (2004); S. Y. Chung, *Appl. Phys. Lett.* **87**, 052901 (2005).

<sup>13</sup>T. T. Fang and H. K. Shiao, *J. Am. Ceram. Soc.* **87**, 2027 (2004).